SAND2017-12553J

Unraveling the semiconducting/metallic discrepancy in $Ni_3(HITP)_2$

Michael E. Foster[1], Karl Sohlberg [2] and …
1. Sandia National Laboratories, Livermore, CA 94551-0969
2. Department of Chemistry, Drexel University, Philadelphia, PA 19104

Abstract

Ni_3(2,3,6,7,10,11-hexaiminotriphenylene)$_2$ is a π-stacked layered metal-organic framework material with extended π-conjugation that is analogous to graphene. Published experimental results indicate that the material is semiconducting, but all theoretical studies to-date predict the bulk material to be metallic. Given that previous experimental work was carried out on specimens containing complex nanocrystalline microstructures, and the tendency for internal interfaces to introduce transport barriers, we apply DFT to investigate the influence of internal interface defects on the electronic structure of bulk $Ni_3(HITP)_2$. The results show that interface defects can introduce a transport barrier by breaking the π-conjugation, and/or decreasing the dispersion of the electronic bands near the Fermi level. Both types of defect open a small gap, in the range of 15-200 meV, in the direction of the defect, which is consistent with the experimentally inferred hopping barrier.

Introduction:

The discovery of graphene[1], and subsequent recognition of its unique electrical and mechanical properties, has spawned great interest in identifying analogous 2D materials that are more amenable to chemical modification and device fabrication [2-4]. One promising recent addition to the set of such graphene analogues is, Ni_3(2,3,6,7,10,11-hexaiminotriphenylene)$_2$, (Ni_3(HITP)$_2$)[5]. In bulk form, Ni_3(HITP)$_2$ is a π-stacked layered material with extended π-conjugation. This highly π-conjugated material has low electron and hole effective masses[6] indicative of a material with high conductivity. Previous theoretical studies, based on first-principles density functional theory (DFT) calculations, predicted the material to be metallic[6-8]. Nevertheless experimental conductivity versus temperature data indicates that the material is semiconducting[5], (with a room temperature conductivity of ~40 S cm^{-1}). One could dismiss the discrepancy between theory and experiment as a consequence of the known tendency of DFT to underestimate the band gap of semiconductors,[9] but several observations suggest that this explanation is incorrect. DFT predicts the absence of a band gap for a variety of exchange-correlation (XC) functionals (PBE, B3LYP, HSE06, and PBE0)[6]. Although XC functionals, based on the generalized gradient approximation (GGA), tend to underestimate band gaps, traditional and screened hybrid functionals have proven much more accurate in this area[10]. In fact, Matsuda et al.[11] found that DFT/B3LYP predicts band gaps accurate to within a remarkable 6 meV of experimental values for single-walled carbon nanotubes (SWCNTs), systems that share similar geometric and electronic structure features with Ni_3(HITP)$_2$. Additionally, the prediction that Ni_3(HITP)$_2$ is metallic remains unchanged for interlayer separations in the range [<3.2 - 3.8 Å] so, the discrepancy is not related to measured/predicted interlayer separation [6]. A similar observation can be made regarding the layer-layer displacement, where the DFT predicted optimal displacement [1.37 Å] lies in the middle of a wide range of displacements [0 - 3.9 Å] over which the material is predicted to be metallic[6]. (See also Fig. 4 below.) These observations prompted us to look elsewhere to understand the (apparent) discrepancy between theory and experiment.

Experimental evidence of the semiconducting nature of Ni_3(HITP)$_2$ is three-fold. First, the reported UV/vis photoabsorption spectrum is suggestive of an onset ca. 0.2-0.3 eV[5]; the spectrum is not definitive because no data are available below 0.4 eV. A second, and more convincing, piece of evidence of the semiconducting nature of the material is its temperature dependence of conductivity, also from Ref.[5] The data show a monotonic increase in conductivity with increasing temperature over the range 75-450 °C, with essentially no hysteresis upon thermal cycling. This thermal dependence of conductance is a signature of the presence of a charge hopping barrier. Finally, the material has been used, as the active channel material, in a field-effect-transistor (FET) and reported to be a p-type semiconductor.[12]

A potentially important clue to the origins of the experimentally inferred band gap in Ni_3(HITP)$_2$ comes from transmission electron micrographs (TEM) taken by Sheberla et al[5]. Under a magnification of ~3500x, the TEM show features that look like pebbles resting on sand with characteristic size of ~1 μm. Atomic force microscopy (AFM) shows roughness with a similar characteristic length scale. From TEM under greater magnification (~20000x) these "pebbles" look like pumice with ridges and cavities having

characteristic features sized on the order of 100 nm. Given this morphology, it is clear that conductance measurements have not been carried out on well-formed single crystals. It is therefore plausible, (we argue likely) that the reported conductive properties of $Ni_3(HITP)_2$ were governed by imperfections in its microstructure, specifically internal interfaces. Two related phenomena support this hypothesis: First, transport in conducting polymers are primarily governed by *inter*-chain hopping, even when the individual chains possess high conductivity due to extended conjugation.[13] In a real sample of conducting polymer material, all of the chains are finite so the charges must eventually hop between chains and consequently the rate-controlling step in charge transport is inter-chain hopping. Second, in crystalline polyacenes, the individual molecular monomers are highly conjugated and presumably highly conductive, but the overall charge transport is governed by *inter*-monomer hopping processes,[14] especially hopping across interfaces (i.e. grain boundaries) as observed in rubrene.[15]

Interfaces[16,17] and defects[18] are well known to lead to transport barriers in materials, but they are often neglected in theoretical and computational work. This neglect is due, in part, to the computational challenge presented by the large size of the unit cell typically required for modeling an internal interface or defect. In this work we apply DFT to investigate the influence of interface defects on the electronic structure of bulk $Ni_3(HITP)_2$. The results show that although the pristine material is metallic, the presence of defects break the electron delocalization and introduces a band gap on the order of 15-200 meV. Moreover, we show that the presence of one type of defect can lead to a large non-optimal displacement of one layer of material relative to an adjacent layer, which can also open a small gap between the valance and conduction bands. Any real sample of material is therefore very likely to possess semiconducting behaviors, which is consistent with the experimentally observations.

Results and discussion:

Figure 1 shows a schematic of a 3×3 supercell extracted from bulk $Ni_3(HITP)_2$; here the characteristic honeycomb lattice is observed. In the idealized bulk material, the layers are π-π stacked 3.3 Å apart, and theory predicts that each layer is offset by $\frac{1}{16}\vec{a}$ (i.e. 1.37 Å in-plane) from the adjacent layer[6]. Although x-ray data is insufficiently detailed to reveal the exact layer-layer offset, the predicted powder pattern based on a structure with a layer-layer offset of $\frac{1}{16}\vec{a}$ is consistent with the observed powder pattern[5,6]. In addition, the results suggest that the layers are disordered, meaning the material lacks long-range-order, a finding that supports this work.

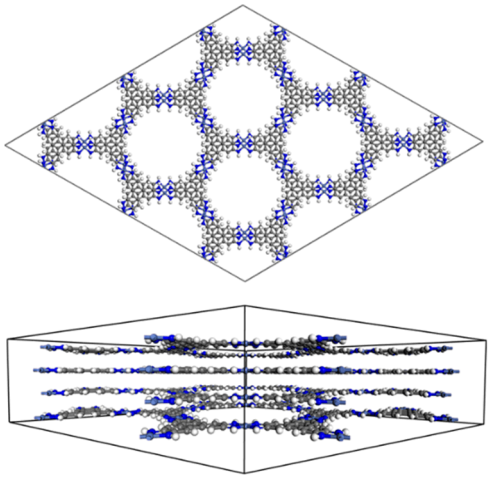

Figure 1. Schematic of a 3×3 supercell of bulk $Ni_3(HITP)_2$.

To investigate the interfacial electronic properties, models of three interface defects were constructed. These are shown schematically in Fig. 2. (See Figs. S1, S2 and S3 in the SI for actual supercell images.) The first (Fig. 2a) is a perpendicular grain boundary in which two grains meet with their layers perpendicular. The second (Fig. 2b) can be described as a strike-slip fault, in which the material is fractured and one grain is slipped in-plane with respect to the other. The third (Fig. 2c) is a layer-layer displacement defect (stacking fault) in which one layer (or more) is slipped in-plane so that its displacement with respect to the adjacent layer(s) is non-ideal.

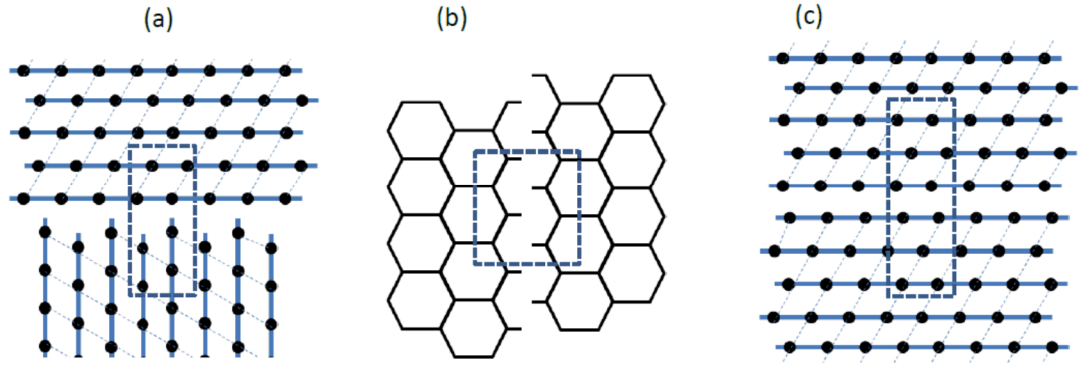

Figure 2. Schematic diagrams of the three interface defect structures studies here. (a) Perpendicular grain boundary. (b) strike-slip fault between grains. (c) layer-layer displacement defect. Images are schematic and intended only to indicate the nature of each interface defect. See Figs. S1, S2 and S3 in the SI for actual supercell images.

A central feature of the interface models, 2a and 2b, is that the extended in-plane π conjugation is broken at the interface. A natural consequence of this disruption in the conjugation is that there is no band dispersion (electron momentum) in the direction normal to the interface. This is confirmed by the band structure shown in Fig. 3. In both interface models, the plane of the interface is perpendicular to

the x-direction. For both models, the band structure exhibits no dispersion along the G-X path. Moreover, the Fermi energy is essentially coincident with the energy of a dispersionless occupied band and the next band along the G-X direction is $150 - 200$ meV higher in energy.

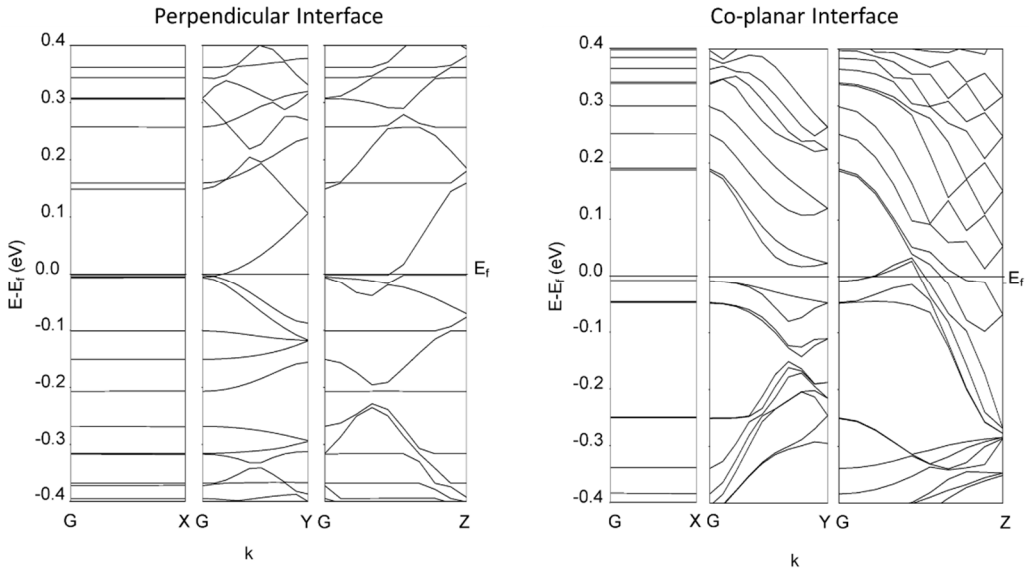

Figure 3. Interface band structure. LHS - perpendicular interface (See Fig. 2a.); RHS co-planar interface (See. Fig. 2b.)

Electronic structure calculations on model 2c (layer-layer displacement defect) reveals two important details. First, the total energy surface, which exhibits a minimum at a displacement of $\frac{1}{16}\vec{a}$, is quite flat in the vicinity of this minimum so that displacements from the optimal offset typically involve a low energy cost. Figure 4a shows a contour map of the total energy as a function of the layer-layer displacement. Second, although theory predicts that the ideal material has no band gap, the introduction of a layer-layer displacement defect can give rise to a band gap for sufficiently large displacements, (typically > 4 Å). Fig. 4b shows a map of the band gap as a function of displacement. A layer-layer displacement defect of between 4-5Å or 7-11 Å can lead to the opening of a band gap on the order of 20-120 meV, also consistent with the experimentally inferred hopping barrier.

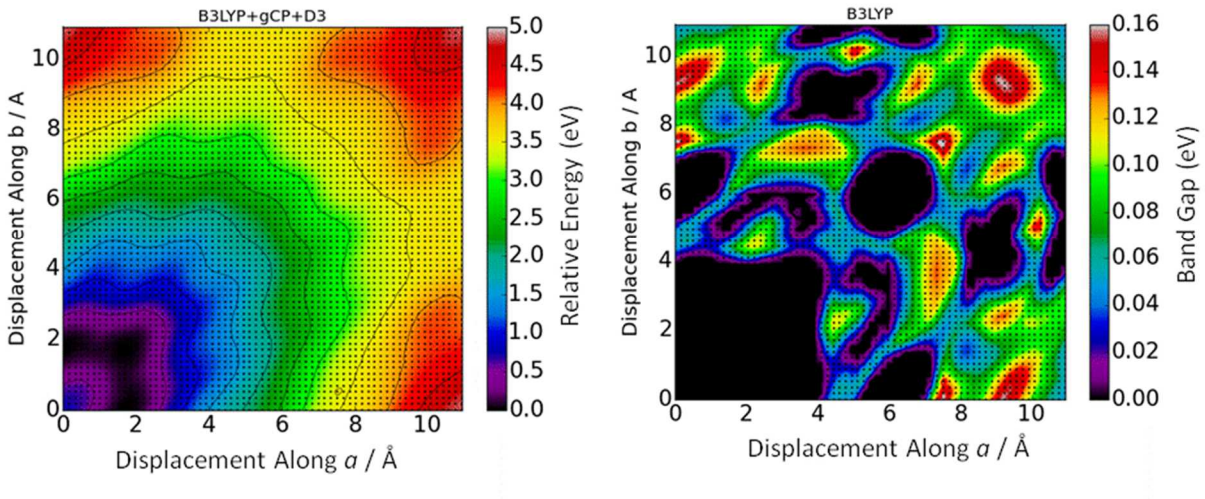

Figure 4. (a) Map of total energy as a function of layer-layer displacement. (b) Map of band gap as a function of layer-layer displacement. Note that the lines $a = 0$, $b = 0$ and $a = b$ are all symmetry equivalent.

Analysis of the electronic structure gives insight into the origins of the observed sensitivity to layer-layer displacement. For such analysis, it is useful to describe the electronic structure of the bulk as arising from the interactions of the electronic structures of the individual sheets of the layered material. The electronic bands near the Fermi level in the bulk material will be composed predominantly of the highest occupied and lowest unoccupied molecular orbitals (HOMO and LUMO). As an infinite stack of layers is brought together to form the bulk, the frontier orbitals interact to produce the bulk bands near the Fermi level. In the simplest approximation, the ensemble of monomer HOMOs form the valance band of the bulk and the ensemble of LUMOs form the conduction band. If the HOMO (LUMO) of an isolated monomer has energy E_H (E_L), and the transfer integral between the HOMOs (LUMOs) of adjacent monomers is given by β , then the valance (conduction) band will span the energy range $E_{vb}=E_H\pm\beta$ ($E_{cb}=E_L\pm\beta'$) as a function of k-space. Roughly speaking, the magnitude of the slope (∂ E/ ∂ k) of band arising from the HOMOs (LUMOs) will be proportional to the magnitude of β (β'). This implies that if the frontier orbitals of adjacent layers are strongly interacting (relatively large $|\beta|$ and $|\beta'|$) then the the valance band maximum (VBM) and conduction band minimum (CBM) will exhibit considerable dispersion, typically leading to a metallic state. In contrast, if the frontier orbitals of adjacent layers are weakly or non-interacting ($|\beta| \approx 0$ and $|\beta'| \approx 0$) the VBM and CBM will exhibit little if any dispersion leading to flat bands and a band gap. (Note, the HOMO/LUMO transfer integrals as a function of displacement are reported in the SI.)

This feature of the electronic structure is confirmed by the band structure illustrated in Figure 5a. of $\frac{1}{16}\vec{a}$. The strongly dispersive band structure in the G-Z direction is clearly evident. Figure 5b shows the band structure when a single layer among a stack of 10 layers is non-optimally shifted, $\frac{27}{64}\vec{a}$. Note the bands are nearly flat along the G-Z path and a gap begins to form at E_f. This effect is even more

pronounced when a group of 5 layers is shifted, 5c, and persists for randomly optimal shifted layers as well, 5d. (Note, in the randomly optimal shifted system all the layers a shifted $\frac{1}{16}\vec{a}$ from each other in random directions; this structure is predicted to be lower in energy structure then the AB stacked material, in agreement with the XRD data[5] indicating that there is no long-range-order.) This flattening of the bands along the G-Z direction opens a gap as large as 100 meV.

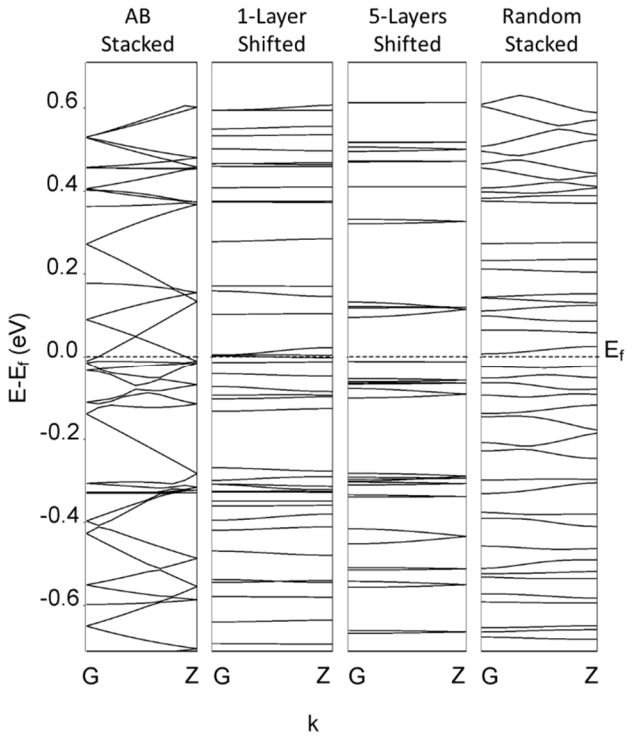

Figure 5. Band structure plots, G-Z, for (a) optimally displaced (AB stacking), (b) 1-layer and (c) 5-layer non-optimally displaced and (d) randomly optimal displaced structures (see SI for complete band structures).

All three interface defects and even optimal random layer displacements, are seen to lead to low-dispersion bands along a path perpendicular to the defect, which tend to open a band gap along that path. It is also important to note that these defects can be inter-dependent, with one kind of defect necessarily introducing a defect of another type. A specific example is shown in Fig. 6. The upper part of the figure shows a top-down view of a monolayer of the material containing a strike-slip fault defect. The lower part of the image shows a top-down view of a bilayer of the material in which one of the layers contains a strike-slip fault. Note that the introduction of the strike-slip fault in one layer of the material forces the presence of a layer-layer displacement in half the material. A consequence of this simultaneous presentation of defects of different types is that a single defect, which opens a band gap in one direction, can force the appearance of another type of defect that opens a band gap in a perpendicular direction as well. This implies that the formation of a single defect can break the

conjugation pathway within the bulk, drastically reducing electron momentum, and introduce a hopping barrier.

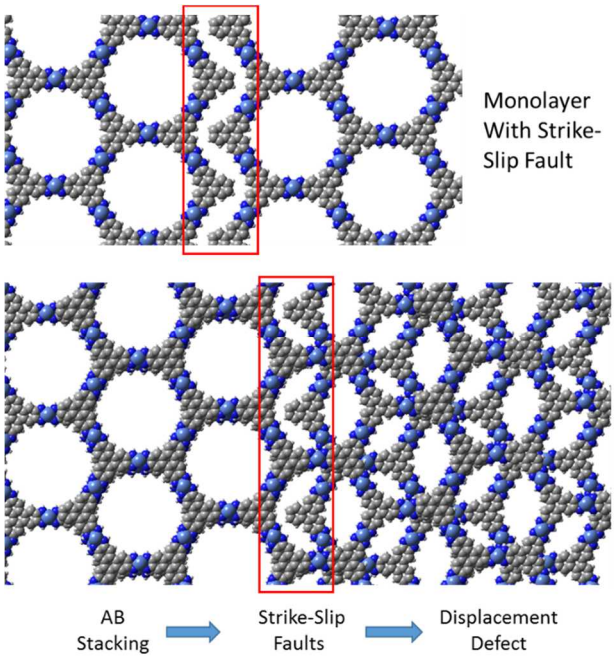

Figure 6. A strike-slip fault in a monolayer (top) forces the presence of a layer-layer displacement defect when present in a bilayer (bottom).

For comparison to experiments, we analyzed the conductivity versus temperature data for bulk $Ni_3(HITP)_2$ presented in Figure 4 of the work by Sheberla.[5] From this data we generated a plot of *ln*(Conductivity) versus ($T^{-0.25}$), (See SI Fig. S5.) The resulting plot is strikingly linear, with an R^2 of 0.983, indicating that the conductivity properties can be represented by the Mott variable-range hopping model.[19,20] (R^2 improves to 0.99 when the temperature range is restricted to 76 - 200 C or 200 - 450 C.) In addition, we estimated the activation energy, by plotting the data in an Arrhenius fashion. The activation energy is found to be 6 meV, if the data in the lower temperature range is used, and 25 meV if the data in the higher temperature range (all data 11 meV). In either case, the result suggests a modest hopping barrier. We believe this barrier is a result of defects in the material (specifically grain boundaries or layer-layer displacement defects) and our electronic structure calculations support this contention.

Noting that the reported[5] microscopy images of $Ni_3(HITP)_2$ show the presents of small particle size, an alternative hypothesis for the origin of the observed charge hopping barrier is that the electronic structure is molecular in nature and exhibit a HOMO-LUMO gap, thereby requiring the thermal activation to yield appreciable conductance. To test this hypothesis, we carried out electronic structure calculations on oligomers of small units extracted from $Ni_3(HITP)_2$. We considered stacks of small molecular units to investigate the variation in the band gap as a function of the number of layers. (Full results are shown in the SI Fig. 6.) It was found that the system switches from molecule-like to bulk-like

in nature with ~6 layers when a layer is composed of only a single Ni center. Given that the inter-layer spacing is ~3.3 Å, these calculations show that molecule-like electronic structure will appear only for particles less than 20 Å thick, corresponding to very short stacks of tiny flakes of the material. It therefore seems clear that particle size is not at the root of the observed hopping barrier since TEM of actual samples shows roughness on a much greater length scale.

In summary, first-principles hybrid DFT calculations of the band structures of interface models of $Ni_3(HITP)_2$ show that the presence of an interface defect can lead a gap at the Fermi level in the direction of the defect. Perpendicular grain boundaries and strike-slip faults defects break the π-conjugation, results in dispersionless bands, and leads to an energy separation of the bands above and below the Fermi energy of 15-200 meV along the direction of the interface (G-X). A layer-layer displacement defect can similarly lead to bands that are nearly dispersionless perpendicular to the stacking direction (G-Z), resulting in a band gap as large as 100 meV. It is further shown that these types of defects can be inter-related; a strike-slip fault leads to the presence of a layer-layer displacement defect. These results are in general agreement with the experimental results. Specifically: measurements of the thermal dependence of conductivity lead to a predicted activation energy in the range of 5.7 to 29 meV. We conclude that although extended conjugated sheets of $Ni_3(HITP)_2$ are highly conducting and the ideal pristine material has a metallic electronic structure, the *overall* conductivity is governed by charge hopping within the microstructure because the presence of defects such as grain boundaries and non-optimal layer-layer displacements. This provides a plausible explanation for the apparent disagreement between theoretical calculations, (which have invariably predicted $Ni_3(HITP)_2$ to be metallic) and experimental work, (which suggests the material is semiconducting). Our work highlights the importance of modeling the microstructure, in addition to the bulk electronic structure, for reliable modeling of electronic properties.

Models and Methods:
Structural models and details of the electronic structure calculations (DFT/B3LYP/pob-TZVP level of theory) are given in the SI. All geometric and electronic structure calculations were performed using Crystal14;[21] except, the HOMO/LUMO transfer integrals, which were calculated (B3LYP/6-31G(d,p) level of theory) using the molecular orbitals and overlap matrices predicted at the gamma-point for a 2D bilayer; these calculations were carried out from data generated within Gaussian 09.

Acknowledgements:

Sandia National Laboratories is a multimission laboratory managed and operated by National Technology & Engineering Solutions of Sandia LLC, a wholly owned subsidiary of Honeywell International, Inc., for the U.S. Department of Energy's National Nuclear Security Administration under contract DE-NA0003525.

References:

1 Novoselov, K.S., Geim, A.K., Morozov, S.V., Jiang, D., Zhang, Y., Dubonos, S.V., Grigorieva, I.V., & Firsov, A.A., Electric Field Effect in Atomically Thin Carbon Films. *Science* **306** (5696), 666-669 (2004). http://dx.doi.org/10.1126/science.1102896

2 Garaj, S., Hubbard, W., & Golovchenko, J.A., Graphene synthesis by ion implantation. *Applied Physics Letters* **97** (18), 183103 (2010). http://dx.doi.org/doi:http://dx.doi.org/10.1063/1.3507287

3 Kwak, J., Chu, J.H., Choi, J.-K., Park, S.-D., Go, H., Kim, S.Y., Park, K., Kim, S.-D., Kim, Y.-W., Yoon, E., Kodambaka, S., & Kwon, S.-Y., Near room-temperature synthesis of transfer-free graphene films. *Nat Commun* **3**, 645 (2012)

4 Kiraly, B., Iski, E.V., Mannix, A.J., Fisher, B.L., Hersam, M.C., & Guisinger, N.P., Solid-source growth and atomic-scale characterization of graphene on Ag(111). *Nat Commun* **4** (2013)

5 Sheberla, D., Sun, L., Blood-Forsythe, M.A., Er, S., Wade, C.R., Brozek, C.K., Aspuru-Guzik, A., & Dinca, M., High Electrical Conductivity in Ni_3(2,3,6,7,10,11-hexaiminotriphenylene)$_2$, a Semiconducting Metal-Organic Graphene Analogue. *Journal of the American Chemical Society* **136** (25), 8859-8862 (2014). http://dx.doi.org/10.1021/ja502765n

6 Foster, M.E., Sohlberg, K., Spataru, C.D., & Allendorf, M.D., Proposed Modification of the Graphene Analogue $Ni_3(HITP)_2$ To Yield a Semiconducting Material. *The Journal of Physical Chemistry C* **120** (27), 15001-15008 (2016). http://dx.doi.org/10.1021/acs.jpcc.6b05746

7 Chen, S., Dai, J., & Zeng, X.C., Metal-organic Kagome lattices M_3(2,3,6,7,10,11-hexaiminotriphenylene)$_2$ (M = Ni and Cu): from semiconducting to metallic by metal substitution. *PCCP Phys. Chem. Chem. Phys.* **17** (8), 5954-5958 (2015). http://dx.doi.org/10.1039/c4cp05328a

8 Zhao, B., Zhang, J., Feng, W., Yao, Y., & Yang, Z., Quantum spin Hall and Z_2 metallic states in an organic material. *Physical Review B* **90** (20), 201403 (2014)

9 Johnson, K.A. & Ashcroft, N.W., Corrections to density-functional theory band gaps. *Physical Review B* **58** (23), 15548-15556 (1998)

10 Moussa, J.E., Schultz, P.A., & Chelikowsky, J.R., Analysis of the Heyd-Scuseria-Ernzerhof density functional parameter space. (2012).

11 Matsuda, Y., Tahir-Kheli, J., & Goddard, W.A., Definitive Band Gaps for Single-Wall Carbon Nanotubes. *The Journal of Physical Chemistry Letters* **1** (19), 2946-2950 (2010). http://dx.doi.org/10.1021/jz100889u

12 Wu, G., Huang, J., Zang, Y., He, J., & Xu, G., Porous Field-Effect Transistors Based on a Semiconductive Metal-Organic Framework. *Journal of the American Chemical Society* **139** (4), 1360-1363 (2017). http://dx.doi.org/10.1021/jacs.6b08511

13 Conchuir, B.O., Tarantini, C., McNeill, C.R., Hüttner, S., & Zaccone, A., Chain-Assisted Charge Transport in Semicrystalline Conjugated Polymers. *The Journal of Physical Chemistry C* **120** (27), 14539-14548 (2016). http://dx.doi.org/10.1021/acs.jpcc.6b04714

14 Deng, W.-Q. & Goddard, W.A., Predictions of Hole Mobilities in Oligoacene Organic Semiconductors from Quantum Mechanical Calculations. *J. Phys. Chem. B* **108**, 8614-8621 (2004). http://dx.doi.org/10.1021/jp0495848

15 Podzorov, V., Menard, E., Borissov, A., Kiryukhin, V., Rogers, J.A., & Gershenson, M.E., Intrinsic Charge Transport on the Surface of Organic Semiconductors. *Physical Review Letters* **93** (8), 086602 (2004)

16 Johnson, K.D. & Dravid, V.P., Grain boundary barrier breakdown in niobium donor doped strontium titanate using in situ electron holography. *Applied Physics Letters* **74** (4), 621-623 (1999). http://dx.doi.org/doi:http://dx.doi.org/10.1063/1.123184

17 Kim, M., Duscher, G., Browning, N.D., Sohlberg, K., Pantelides, S.T., & Pennycook, S.J., Nonstoichiometry and the Electrical Activity of Grain Boundaries in $SrTiO_3$. *Phys. Rev. Lett.* **86**, 4056 (2001)

18 Cretu, O., Krasheninnikov, A.V., Rodriguez-Manzo, J.A., Sun, L., Nieminen, R.M., & Banhart, F., Migration and Localization of Metal Atoms on Strained Graphene. *Physical Review Letters* **105** (19), 196102 (2010)

19 Mott, N.F., Conduction in glasses containing transition metal ions. *Journal of Non-Crystalline Solids* **1** (1), 1-17 (1968). http://dx.doi.org/10.1016/0022-3093(68)90002-1

20 Wexler, R.B. & Sohlberg, K., Models for the Temperature and Gas Partial Pressure Dependence of Conductance. *Reviews in Theoretical Science* **4** (2), 97-111 (2016)

21 Dovesi, R., Orlando, R., Erba, A., Zicovich-Wilson, C.M., Civalleri, B., Casassa, S., Maschio, L., M., F., De La Pierre, M., D'Arco, P., Noel, Y., Causa, M., Rerat, M., & Kirtman, B., CRYSTAL14: A program for the ab initio investigation of crystalline solids. *Int. J. Quantum Chem.* **114**, 1287 (2014)